Microwave Assisted Synthesis of Ag@TiO_2 Nanocomposites: Photoinduced Studies on Methylene Blue under UV Irradiation

G.S.Yashavanth Kumar[1], H.S. Bhojya Naik*[1], R.Vishwanth[1], Ameena Parveen[2], Aashis.S.Roy[3]

Department of Studies and Research in Industrial Chemistry, School of Chemical Sciences, Kuvempu University, Shankaraghatta-577 451, INDIA.
Department of Physics, Govt. First Grade College, Gurmitkal -585214, Karnataka, India
Department of Materials Science, Gulbarga University, Gulbarga -585106, India

Abstract:

Silver cored TiO_2 shell nanocomposites has been prepared by microwave irradiation technique and well characterized. The photocatalytic activity results showed that the photodegradation efficiency of Ag@TiO_2 nanocomposite on methylene blue reached 77.71% under UV irradiation. The effect of photocatalyst and hydrogen peroxide has been studied in the present paper. Finally, the results support the positive effect of silver over TiO_2 on methylene blue may be due to its ability to trap electrons during the degradation processes.

Keywords: Ag@TiO_2 nanocomposite, microwave-irradiation, methylene blue, photocatalysis

Author of correspondence: H.S. Bhojya Naik

1. Introduction

Heterogeneous photo catalysis has attracted extensive attention during the last decades to degrade pollutants. Much effort has concentrated on the important metal oxides such as TiO_2, SnO_2, V_2O_5, and ZnO [1, 2, 3, 4, 5]. Among them, TiO_2 and TiO_2-derived materials are of importance for utilizing solar energy and environmental purification. However, TiO_2 exhibits a relatively high energy bandgap (~3 to 3.2 eV) and can only excited by high energy UV irradiation with a wavelength shorter than 387 nm. Effort have been made to extend the light absorption range of TiO_2 from UV to visible light or to improve the photo catalytic activity of TiO_2 by the use of nanocomposites of TiO_2 with a narrow band semiconductor materials of transition or noble metals. With a higher conduction band than that of TiO_2, these metal not only photosensitize the TiO_2 materials can also induce an efficient and larger charge separation by minimizing the electron-hole recombination. In recent years various attempts have been made to reduce e^--h^+ recombination by doping metal ions in to the TiO_2 lattice and coupling semiconductors to enhance the efficiency of degradation of wide range of organic pollutants in both aqueous and gaseous phase [6-10].

Since, the use of nanomaterials in photodegradation studies has received much attention, the method of preparation of different nanostructured materials are attracted in recent years. Therefore, the author has developed simple, ecofriendly method for the preparation of Ag@TiO_2 nanocomposites. Due to the importance of nanostructured materials in photocatalytic activity, the photodegradation activity studies on methylene blue under UV irradiation is exhibited.

2. Experimental

2.1. Reagents

All the reagents used were analytical grade. $AgNO_3$ of AR grade was purchased from Himedia with 99% purity and ethylene glycol from Sigma Aldrich chemicals. TiO_2 particles used in the experiment were prepared by the reported procedure [11].

2.2. Preparation of $Ag@TiO_2$ Core- Shell nanocomposites

In a typical synthesis of $Ag@TiO_2$ core-shell nanocomposite clusters, TiO_2 particles (0.02 gm) was added to 10 mL of ethylene glycol (EG) containing desired amount of $AgNO_3$ (0.01 gm). The mixture were loaded into the reaction vessel and heated in a microwave (160 W) for 14-15 min. Then, the reaction mixture was cooled to room temperature. The precipitate deposited on the bottom of the vessel was collected, washed with ethanol and dried at 60-80 ^oC for 10 hrs. The reaction pathway is presented in scheme 1.

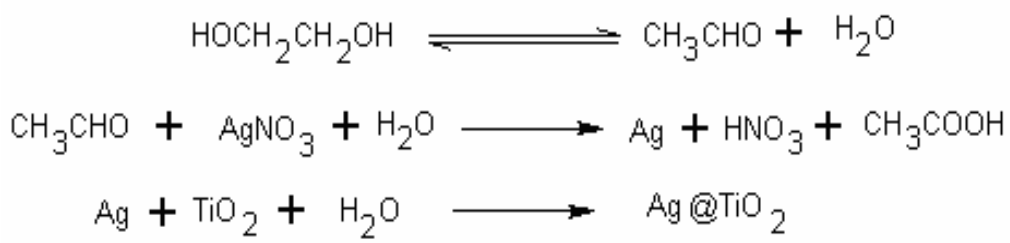

Scheme 1: Reaction pathway in the synthesis of $Ag@TiO_2$ core-shell nanostructures

2.3. Characterization:

The synthesized nanoparticles were characterized by UV-visible spectroscopy , XRD and Scanning electron microscopic technique. The UV-visible spectrum was recorded on UV-visible Spectrophotometer, Shimadzu PC 1650 model. The powder X-ray diffraction (XRD) experiments were carried out at room temperature using X-ray diffractometer (Cu Kα λ = 0.154 nm) to identify the crystal phase of the products. SEM images were obtained at 20 kV.

2.4. Photocatalytic activity:

The photocatalytic degradation was carried out in a photoreactor with irradiation source of UV lamp (15W, UV-C, λ_{max} = 254 nm) which was placed in front of the reactor. During the photocatalytic degradation, the mixture of methylene blue (MB) 100 mL , 60 mg of photocatalyst (TiO_2 and $Ag@TiO_2$ seperately) was quantitatively transferred in to a photoreactor. The prepared suspension was then sonicated for 5 min in the darkness. Then, the lamp was switched on to initiate the reaction. During irradiation, the mixture of solution was stirred to keep the suspension homogenous with magnetic stirrer. The suspension was sampled 30 mins intervals of illumination time. Before determination of concentration of the MB, sample was centrifuged at a rate of 5000 rpm to remove presence of photocatalyst. The concentration of the MB in each degraded sample was determined using a spectrophotometer (UV-visible Spectrophotometer, Shimadzu PC 1650 model) at λ_{max} = 367 nm with calibration curve.

3. Results and Discussion:

Microwave-assisted heating has been shown to be an invaluable technology in the synthesis of nanoparticles. It often dramatically reduces reaction times, typically from days or hours to minutes or even seconds and it can also provide pure products in quantitative yields. In the present work, the mixture of $AgNO_3$, TiO_2 and ethylene glycol was kept in the reaction vessel. The derived $Ag@TiO_2$ nanoparticle was obtained within 15 min of irradiation. Whereas in conventional method, the reaction took 14-15 hrs. In both the methods the reaction proceeds by the reduction of metal ions and coating of TiO_2 particles in ethylene glycol (EG) [12].

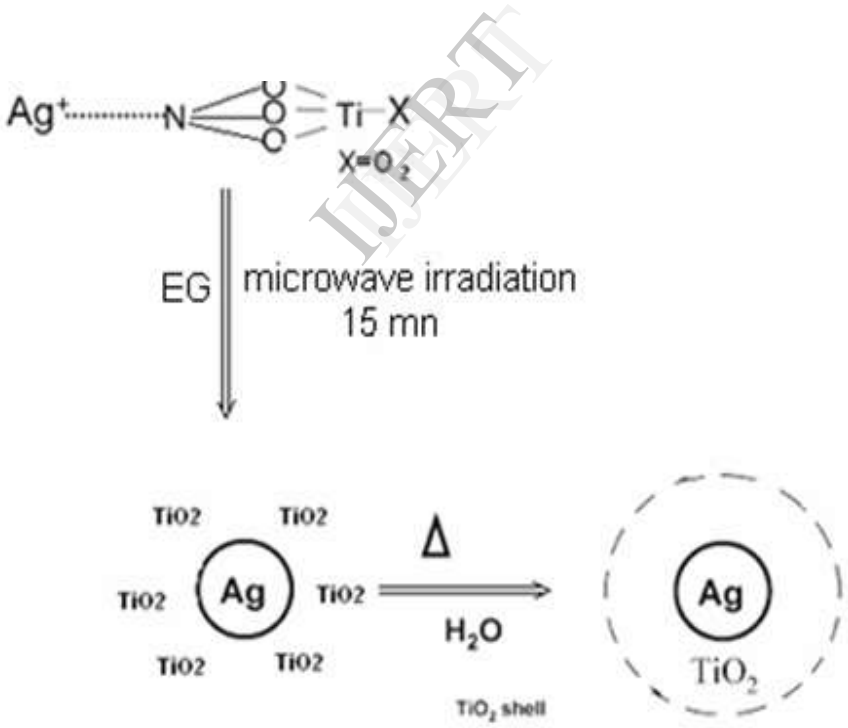

Scheme 2: The formation of $Ag@TiO_2$ core-shell nanostructures

The solvent EG plays an important role over Ag+ ions first, followed by the slow addition of TiO_2 particles to form a shell around the metal core. As the amount of EG increases the primary step of reduction rate of Ag^+ ion to Ag^o increases. It is important that the reduction rate of Ag^+ ion is greater than the rate of formation of TiO_2 shell. After 15 min of irradiation, it was found that the obtained precipitate of core-shell particles was stable. As Ag^+ ions are reduced by EG to form small metal particles, they quickly interact with the TiO_2 nanoparticles. The TiO_2 slowly coated on the surface of Ag particles and yield TiO_2 shell. The formation of core-shell cluster is illustrated in scheme 2.

3.1. SEM Characterization

The morphology of the synthesized Ag@TiO_2 nanostructure was characterized by scanning electron microscopic (SEM) technique. The SEM pictures elucidate the ununiform distribution of TiO_2 nanoparticles on the surface of silver with irregular shaped Ag@TiO_2 particles which are aggregated as tiny crystals as shown in the figure 1.

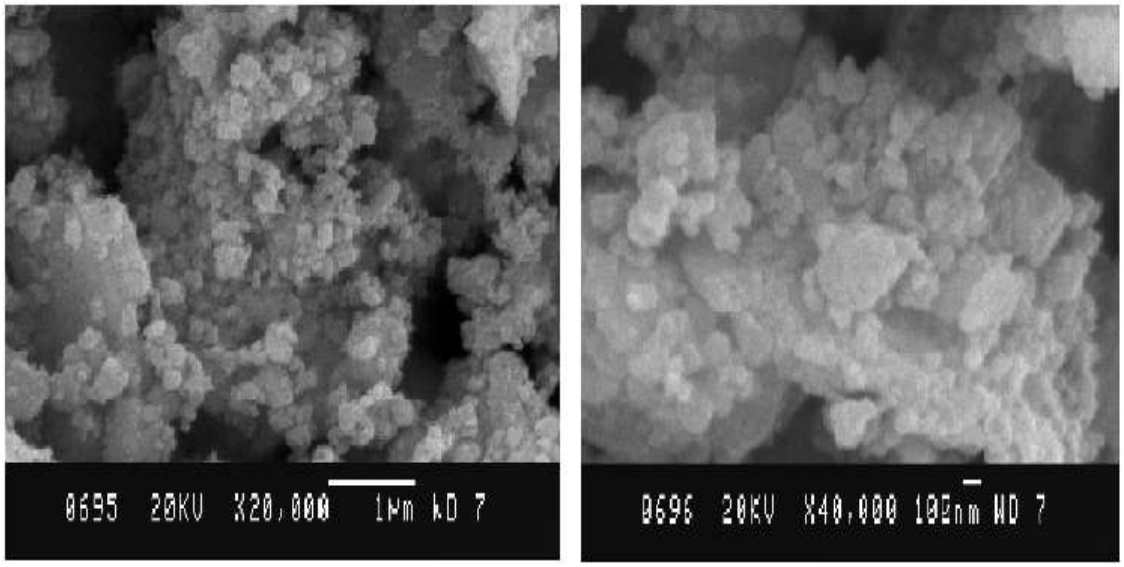

1a **1b**

Fig. 1. SEM images (1a and 1b) of Ag@TiO_2 core-shell nanocomposites

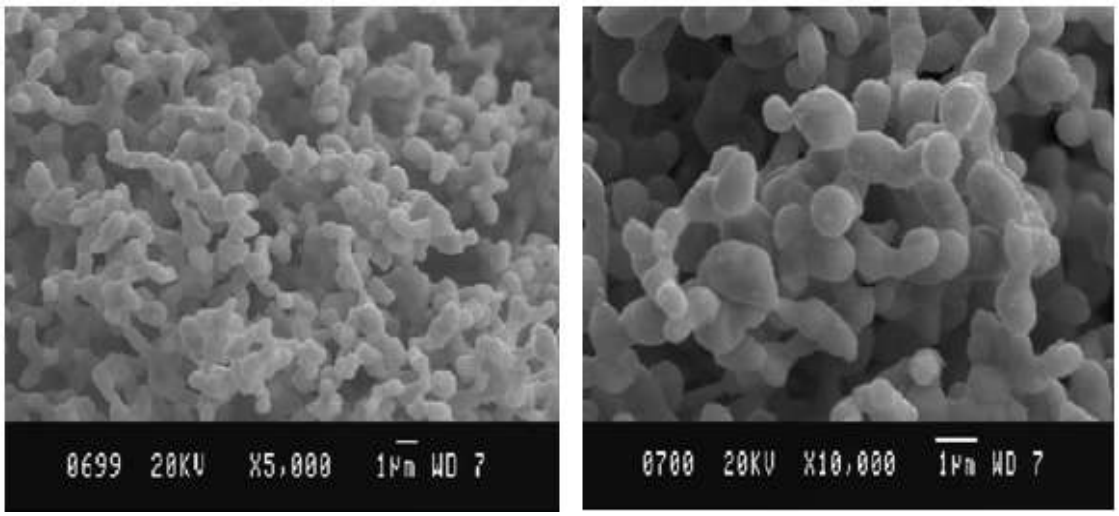

2a **2b**

Fig. 2. SEM images (2a and 2b) of silver nanoparticles synthesized in the absence of TiO_2 nanoparticles

3.2. XRD Analysis

Further to determine the crystal phase composition of the prepared composite, the X-ray diffraction measurements were carried out at room temperature over the diffraction angle of 10-80°. The typical XRD pattern of TiO_2 and $Ag@TiO_2$ composites are shown in the figure 2. The average particle size (D in nm) of $Ag@TiO_2$ nanocomposite is determined from the XRD pattern (Fig 3) according to the Scherrer's equation i.e.,

$$D = \frac{K\lambda}{\beta \cos\theta}$$

(Where, K is a constant equal to 0.89, λ is the X-ray wavelength equal to 0.154 nm, β is the full width at half maximum and θ is the half diffraction angle).

The XRD pattern of $Ag@TiO_2$ nanocomposites shows that the full width at half maximum, β is 0.231 and the half diffraction angle 2θ is 38.123. The XRD data indicates that the size of the $Ag@TiO_2$ nanocomposite is in the order of 36 nm.

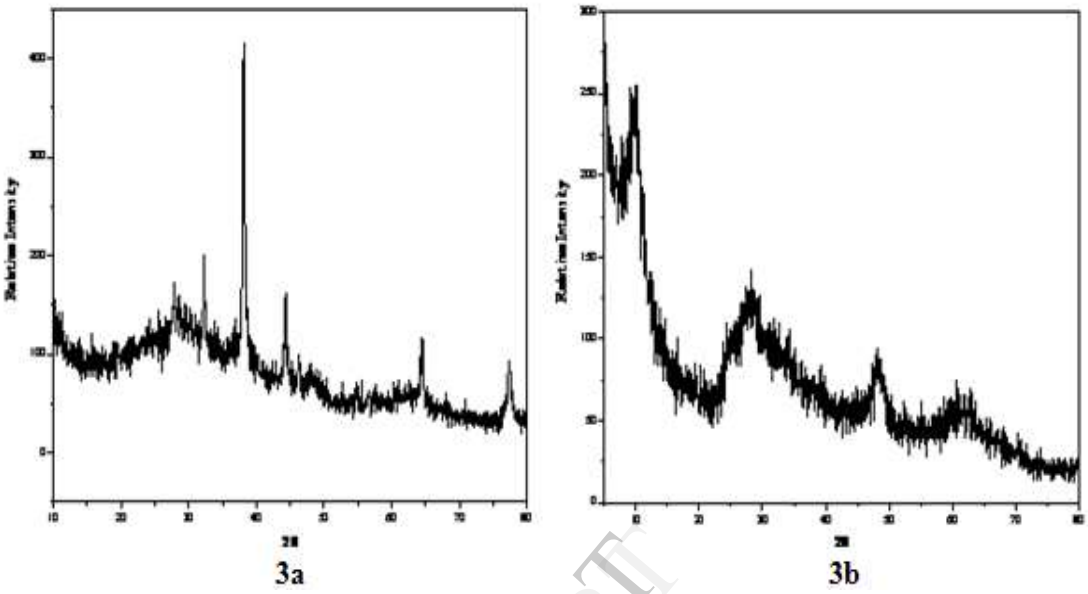

Fig. 3. (a) XRD pattern of $Ag@TiO_2$ core-shell nanocomposites structures and (b) XRD pattern of TiO_2 nanoparticles.

3.3. EDX analysis

To confirm the composition of the products obtained EDX analysis was performed on the $Ag@TiO_2$ core-shell nanocomposites. The survey of EDX spectrum (Figure 4) indicates that the core-shell nanocomposites are mainly composed of Ag, Ti, and O.

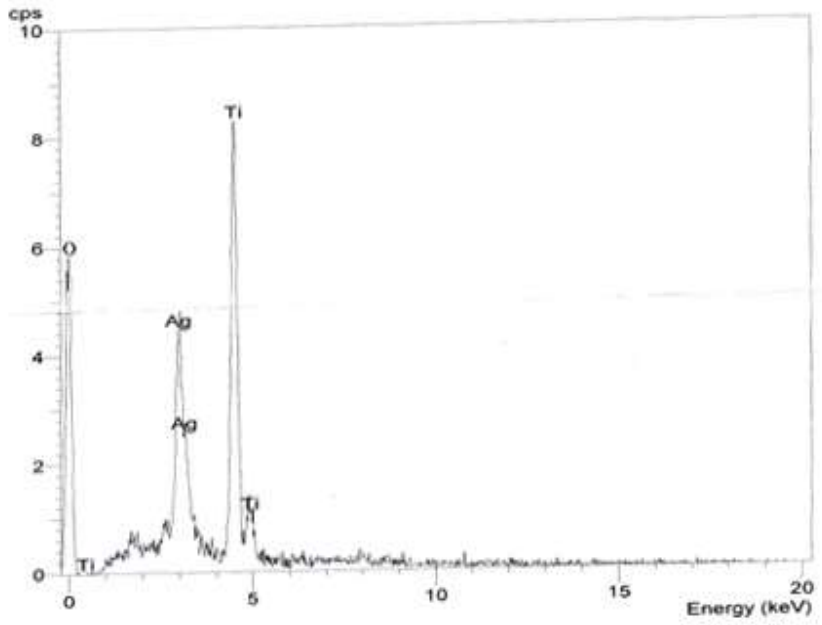

Fig. 4. EDX spectrum of $Ag@TiO_2$ nanocomposites

3.4. UV-visible spectral Analysis

The absorption spectra (Fig 5) were recorded individually for TiO_2 and $Ag@TiO_2$ using Shimadzu PC 1650 model spectrophotometer. The optical response shows that the $Ag@TiO_2$ materials exhibited wide absorption band in the UV-visible region. The absorbance of the pure TiO_2 exhibited sharp absorption bands where as the $Ag@TiO_2$ core-shell particles exhibited wide absorption band with two peaks at 311nm and 319nm**.** The wide absorption peak attributed to the transverse plasmon response of the core silver particles. Obviously, wide bands of newly synthesized samples were significantly red-shifted compared with those of uncoated pure silver particles, verifying that the core-shell motif was formed [13].

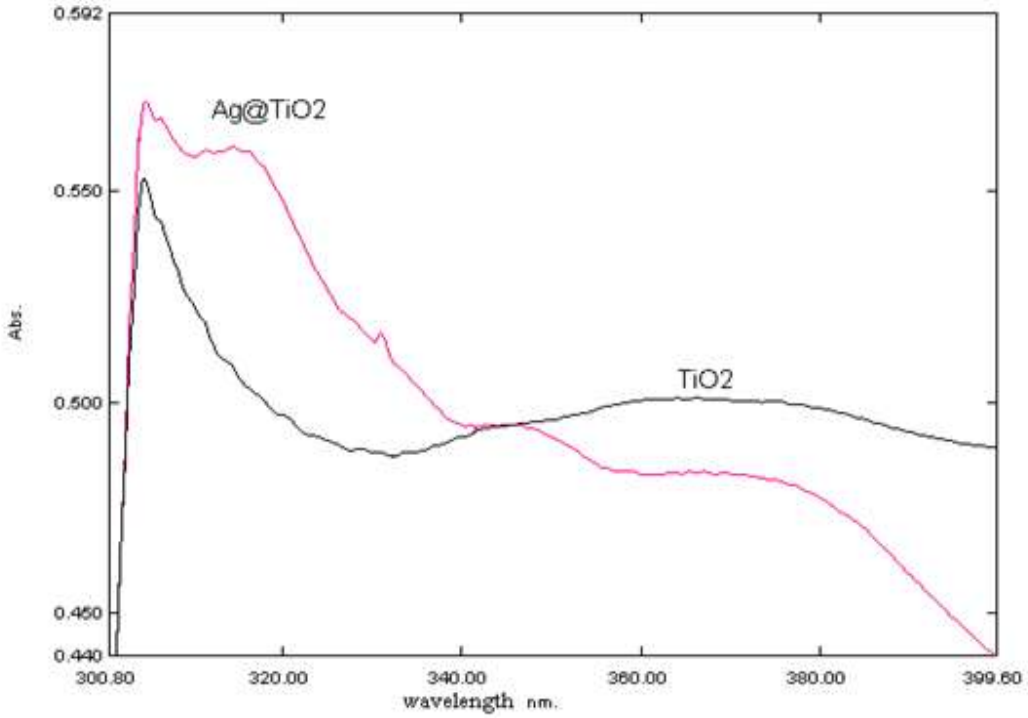

Fig. 5. Absorption spectra recorded following UV-irradiation of TiO_2 and $Ag@TiO_2$ colloidal suspensions in ethanol.

3.5. Photocatalytic activity

The photocatalytic activity of the $Ag@TiO_2$ with that of TiO_2 colloids was compared carrying out the degradation studies using methylene blue (MB) dye. IN general, the initial step in TiO_2 mediated photocatalysis degradation proposed to involves the generation of a (e^-/h^+) pair leading to the formation of hydroxyl radicals ($^{\bullet}OH$) and superoxide radical anions ($O2^{\bullet-}$). These radicals are the oxidizing species in the photocatalytic oxidation processes. The efficiency of the dye degradation depends on the concentration of the oxygen molecules, which either scavenge the conduction band electrons (e_{cb}^-) or prevent the recombination of (e^-/h^+). The electron in the conduction could be picked up by the adsorbed dye molecules, leading to the formation of dye radical anions and the degradation of the dye [14].

The photocatalytic efficiency of TiO_2 and $Ag@TiO_2$ composites on methylene blue (MB) at room condition and on UV irradiation were carried out.

3.5.1. At room condition without UV irradiation

The silver doped TiO_2 nanomaterial showed less degradation activity on MB at room condition without calcinations and UV irradiation. From the figure 6 the $Ag@TiO_2$ nanostructures showed 5.5% decomposition of MB dye presented in figure 6**.**

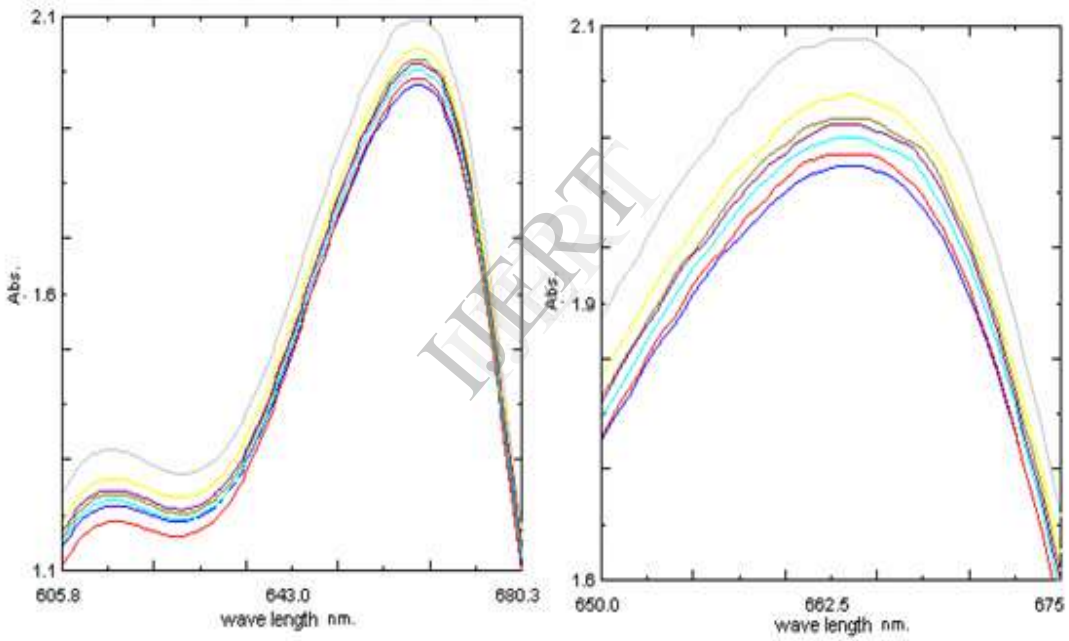

Fig. 6. Photodegradation of MB using $Ag@TiO_2$ core-shell nanoparticles under room condition.

3.5.2. Without calcination under UV irradiation

The figure 7 and 8 shows the change in UV-visible spectra and % degradation of MB dye using $Ag@TiO_2$ core-shell nanoparticles without calcination under UV irradiation. The absorbance decreases from 1.765 to 1.192. From these values, it can

predict that the photocatalytic activity of nanocomposites could be activated by UV irradiation.

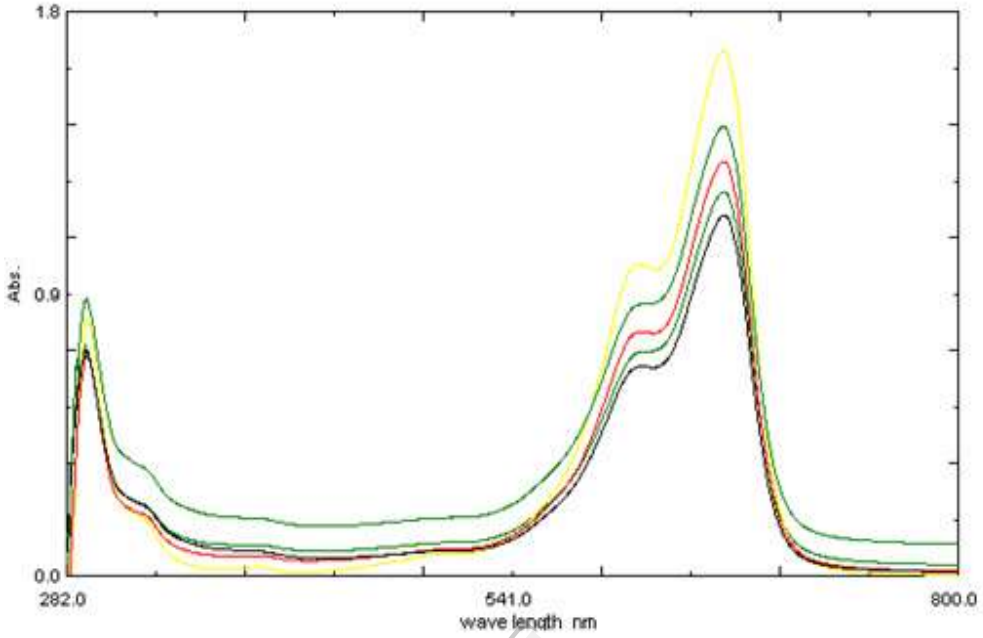

Fig. 7. Photodegradation of MB using Ag@TiO_2 core-shell nanoparticles without calcination under UV irradiation.

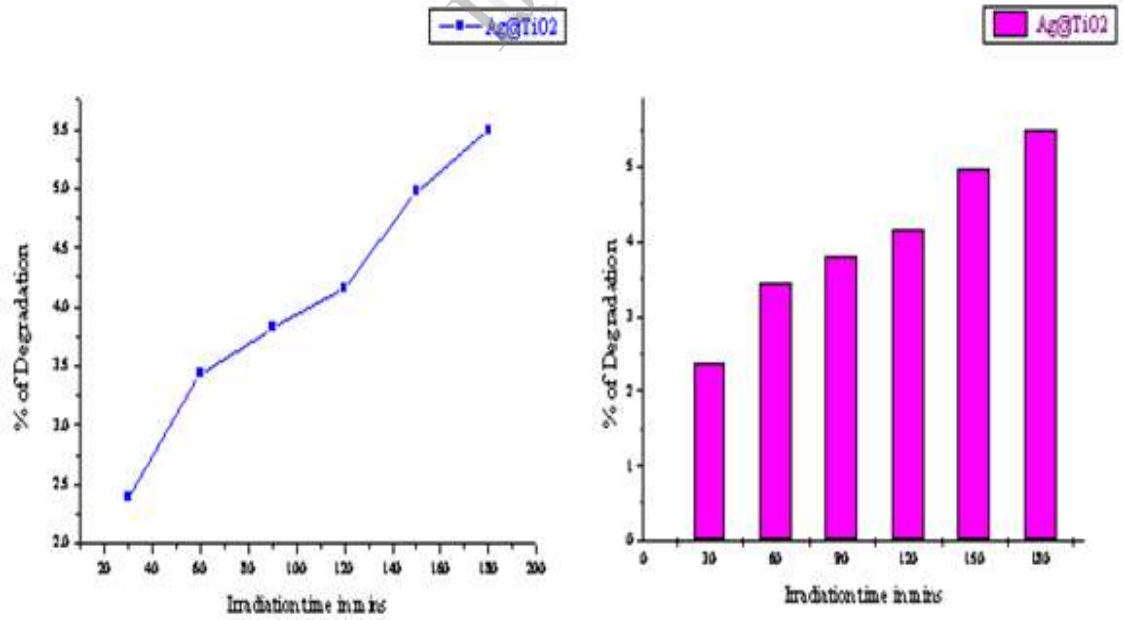

Fig. 8. The % degradation of MB dye using Ag@TiO_2 core-shell nanocomposites without calcination under UV irradiation.

3.5.3. With calcination under UV irradiation

The aqueous solution of the MB dye was a little unstable under UV radiation in absence of TiO_2 [15]. However, the MB dye undergoes very slow degradation in aqueous MB/TiO_2 dispersions upon UV irradiation. The changes of the UV–vis spectra during the photodegradation process of the MB dye in the aqueous TiO_2 and Ag@TiO_2 dispersions under UV irradiation are illustrated in figure 9 and 10. The % of degradation of MB dye was shown in the figure 11.

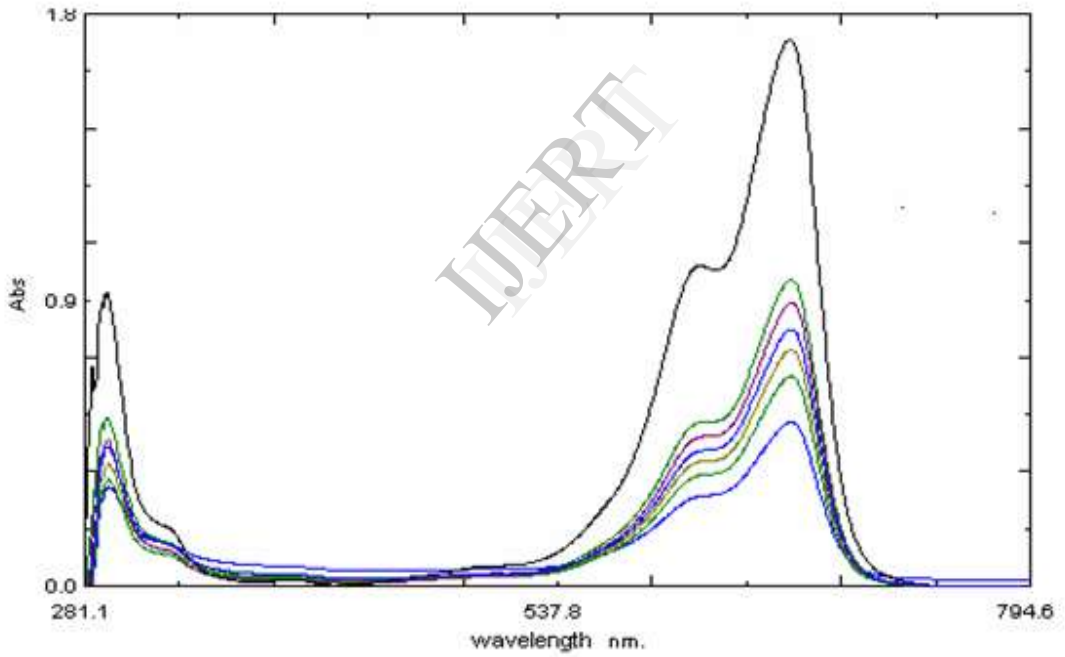

Fig. 9. The change of UV- Visible spectra during the photodegradation process of MB dye in aqueous TiO_2 dispersions under UV irradiations.

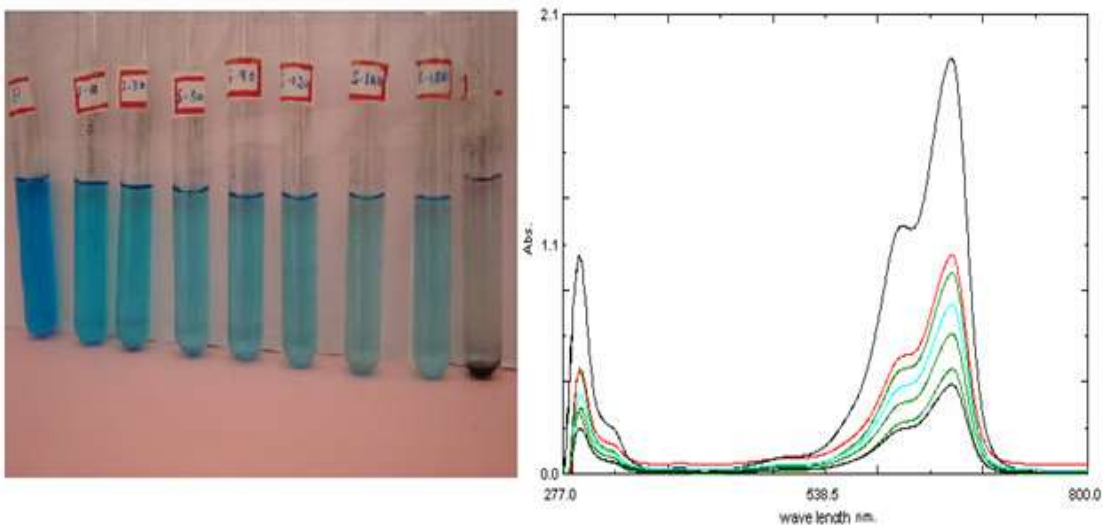

Fig. 10. The change of UV-Visible spectra during the photodegradation process of MB dye in aqueous Ag@TiO_2 dispersions under UV irradiations.

The photocatalysts were activated by calcination at temperature of 200 ^oC for 30 min. During UV irradiation, the characteristic absorption band of the dye at 664 nm decreased rapidly from the absorbance 1.741 to 0.628 for TiO_2 and 1.812 to 0.423 for Ag@TiO_2 after 3 hrs of UV illumination, but their was no shift in wavelength observed. It indicated that the photodegradation mechanism is favorable to cleavage of the whole conjugated chromophore structure of the MB dye in to their fragments. Thus the Ag@TiO_2 composites showed higher photocatalytic efficiency than pure TiO_2. The photodegradation efficiency of MB increases with the increase of Ag amount in the nanocomposites [16]. After three hrs irradiation, the photodegradation efficiency of Ag@TiO_2 reached 77.71%, which was the highest in all samples, where as in the presence of undoped TiO_2 materials, degradation goes up to 69.4% only. The improved photodegradation activity of TiO_2 may be due to the doping of Ag metal on TiO_2 increases the surface of metal oxide and on which the cationic MB dye may adsorbed. It can also explained as; Ag is excited by visible light to produce photoinduced electrons

and holes, followed by electron injection from excited Ag into the conduction band of TiO_2. Then, the reactive electrons from the conduction band of TiO_2 can reduce O_2 to its radical anion O_2^- and OH^- ions into $^{\cdot}OH$, resulting in the oxidation of methylene blue at last. On the other hand, the reactive holes from the covalent band of Ag can also oxidize MB to its radical cation either directly or through a primarily formed OH^- produced by the oxidation of ubiquitous water. Hence, the Ag ion plays an important role in the improvement of photocatalytic efficiency of the $Ag@TiO_2$ nanocomposites and generation of free radicals.

$$Ag\text{-}TiO_2 + e^- \xrightarrow{h\nu} Ag\text{-}TiO_2 + e^-_{CB} + h^+_{VB}$$

$$Ag\text{-}TiO_2 - OH^- + h^+_{VB} \longrightarrow Ag - TiO_2 - OH^{\cdot}$$

$$O_2 + e^- \longrightarrow O_2^-$$

Possible mechanism involved in the degradation of Methylene Blue is illustrated as follows,

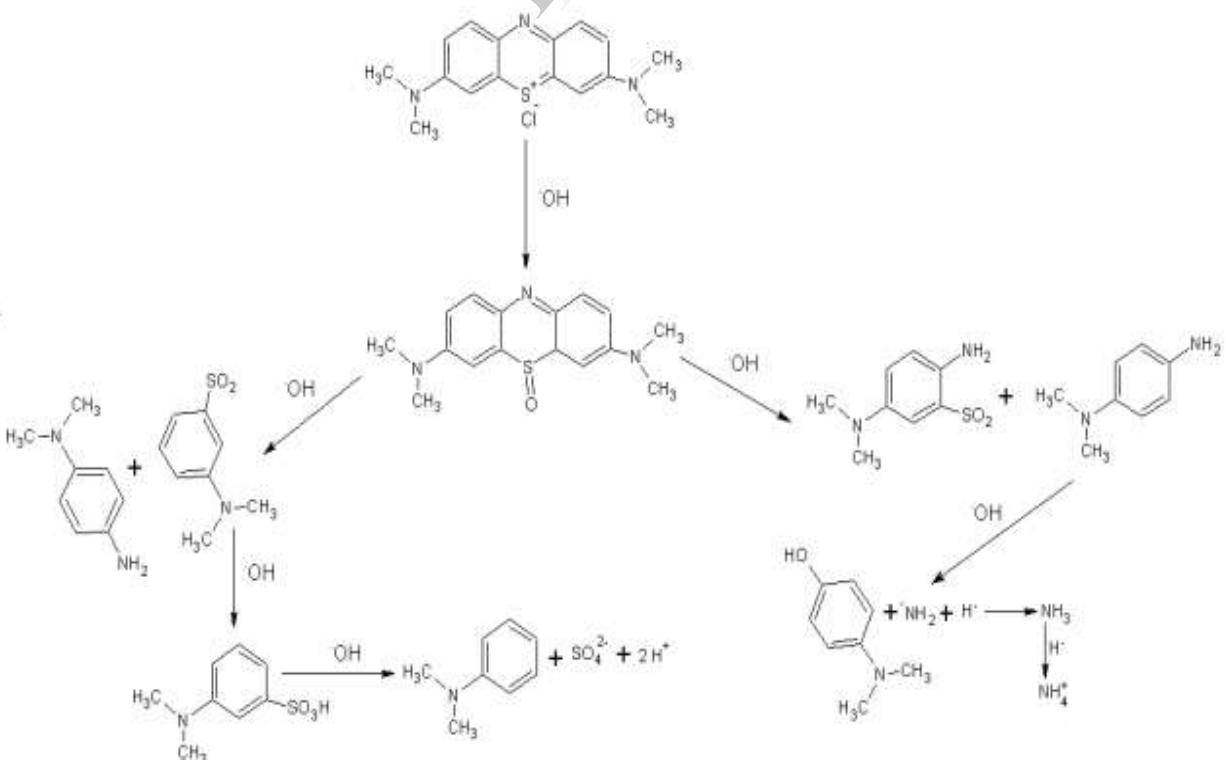

3.5.5 Effect of temperature

In order to study the influence of the calcination temperature on the photocatalytic activity of Ag doped TiO_2, the $Ag@TiO_2$ photocatalyst was calcined at 100, 200, 300, 400 ^oC and results are shown in the figure 12 and 13**.** The results in the figure shows that the absorbance constantly decreased with increasing the calcination temperature, supports the photocatalytic activity of $Ag@TiO_2$ nanocomposites increases with increasing the calcination temperature.

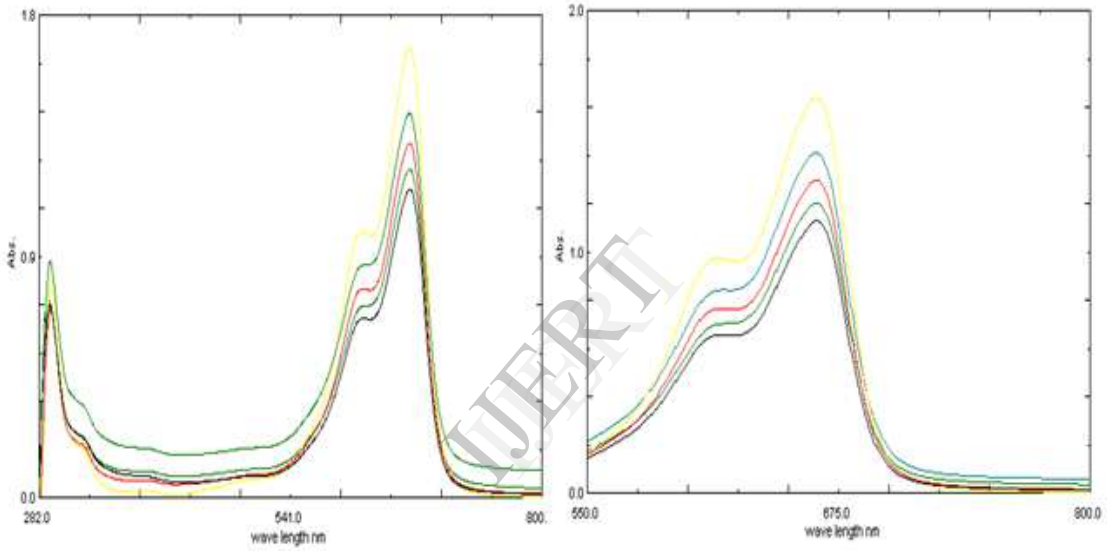

Fig. 12. The effect of calcinations temperature on the photocatalytic activity of Ag doped TiO_2 in the degradation process of MB dye in aqueous medium.

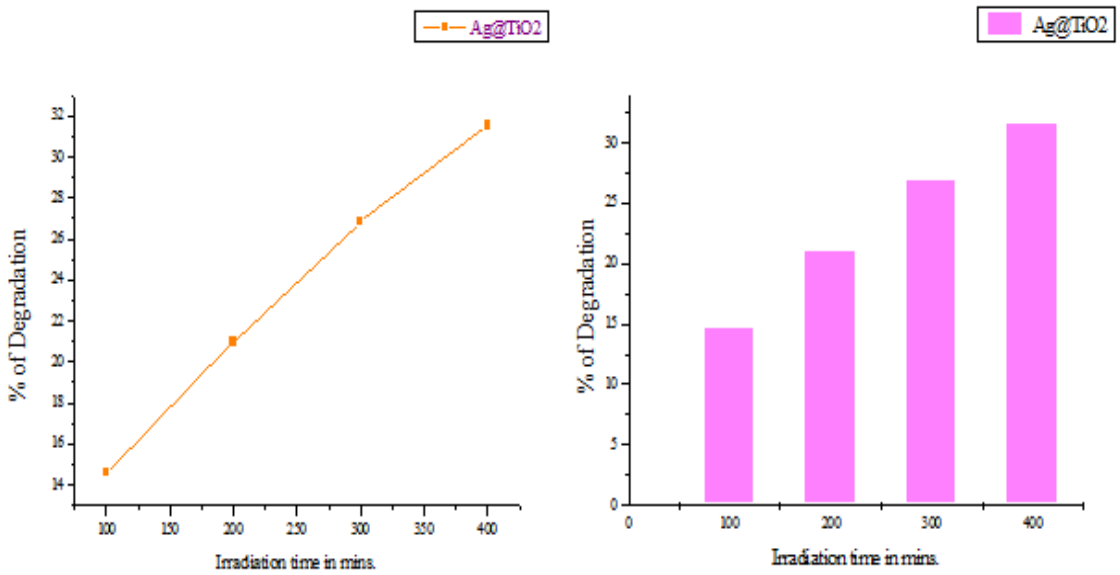

Fig. 13. The effect of calcination temperature on the % degradation of MB dye using Ag@TiO_2 core-shell nanocomposites

3.5.6. Influence of H_2O_2 and Photocatalyst on the degradation of methylene blue dye

The effect of H_2O_2, H_2O_2 and TiO_2 nanoparticles and H_2O_2 and Ag@TiO_2 nanocomposites on the degradation of methylene blue dye under UV irradiations were studied.

The effect of H_2O_2 on the degradation of methylene blue dye was studied at a concentration of 10ml/L under UV irradiation. When we observe the UV visible spectra as shown in the figure 14 their is a hypochromic shift takes place which indicates that number of methylene blue molecule goes on decreasing with increasing the illumination time of UV irradiation. It is evident that the absorbance get decreases from 1.178 Abs to

0.721 Abs after 2.5 hrs of UV illumination. Hydrogen peroxide upon UV irradiation leads to the generation of ˙OH free radicals and these ˙OH radicals are mainly responsible for the degradation of methylene blue dye. Initially the efficiency of degradation of methylene blue in 30 min is more when compared to the degradation process after 2.5 hrs may be due to the presence of more number of ˙OH free radicals. At an illumination time of 2.5 hrs, 58.04 % photocatalytic degradation of methylene blue dye was observed.

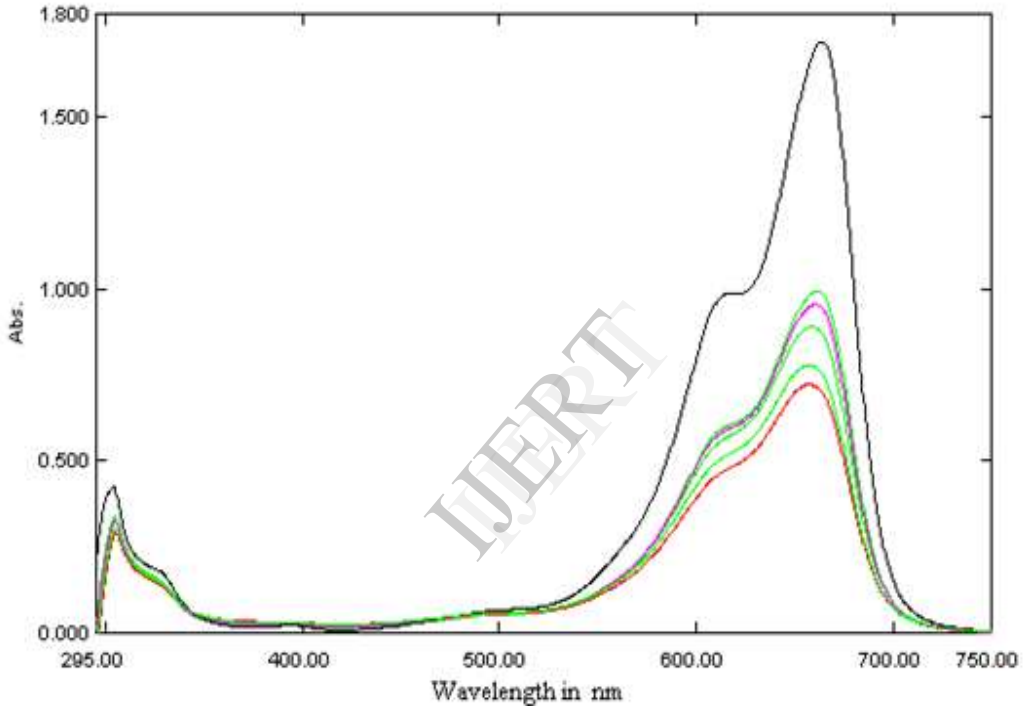

Fig. 14. The change of UV- Visible spectra during the photodegradation process of MB dyes in the presence of H_2O_2 under UV irradiations.

Figure 15 shows the change in the UV-visible spectra obtained during the photocatalytic degradation of methylene blue dye in the presence of H_2O_2 and TiO_2 under UV irradiation. At an illumination time of 2 hrs, 89.12% photocatalytic degradation of methylene blue dye was observed. These observations were due to the electron acceptor behavior of H_2O_2, which reacted with conduction band electrons generated by the

photocatalyst to generate hydroxyl radicals required for the degradation of methylene blue [17].

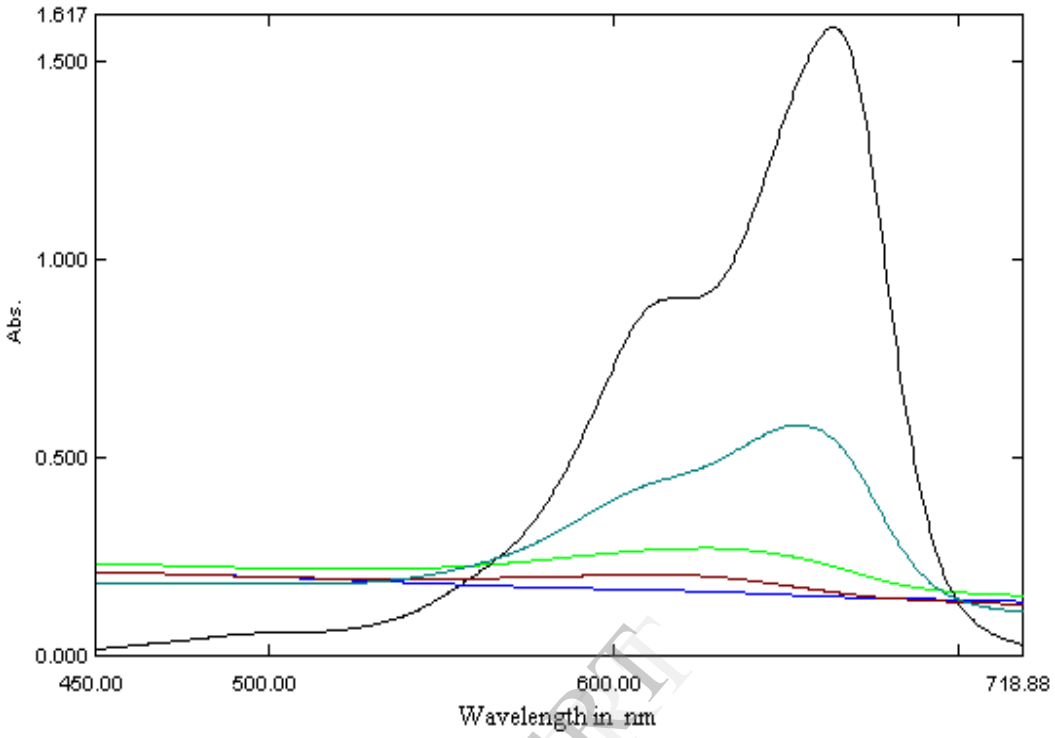

Fig. 15. The change of UV- Visible spectra during the photo degradation process of MB dye in the presence of H_2O_2 and TiO_2 nanoparticles under UV irradiations

Photodegradation study was further carried out in the presence of H_2O_2 and Ag@TiO_2 under UV irradiation. From the figure 16 we can predict that there is no characteristic spectral line for methylene blue dye. It means that the dye molecule completely degraded within 30 min of UV irradiation in the presence of H_2O_2 and Ag@TiO_2 nanocomposites. At an illumination time of 1 hr, 93.7 % photocatalytic degradation of methylene blue dye was observed.

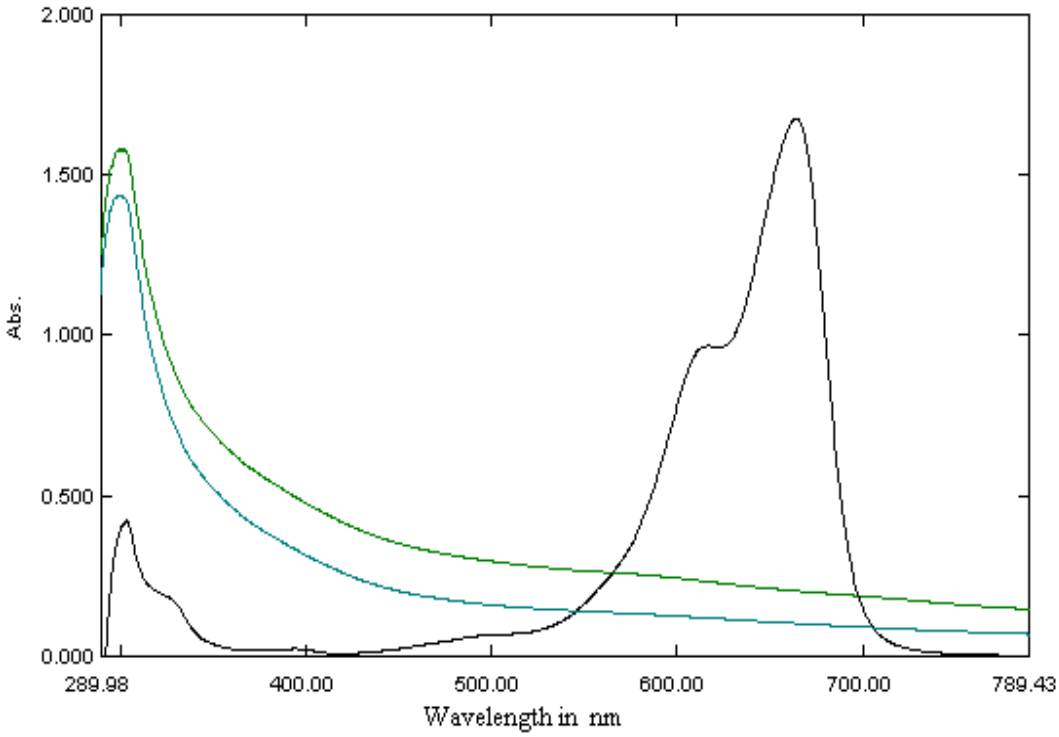

Fig. 16. The change of UV- Visible spectra during the photo degradation process of MB dye in the presence of H_2O_2 and $Ag@TiO_2$ nanocomposites under UV irradiations

From the results obtained these $Ag@TiO_2$ core-shell nanocomposites have the ability to store photogenerated electrons. These electrons are taken up by the H_2O_2 and get dissociated into hydroxyl radicals which are responsible for the degradation of methylene blue molecule.

$$H_2O_2 + e^-_{CB} \longrightarrow {}^{\bullet}OH + {}^{-}OH$$

$$H_2O_2 + \dot{O}_2^- \longrightarrow {}^{\bullet}OH + {}^{-}OH + O_2$$

3.6. Conclusions

In summary, simple ecofriendly has been developed for the preparation of $Ag@TiO_2$ nanocomposite using microwave irradiation. The synthesized $Ag@TiO_2$ nanocomposites were characterized by SEM, XRD and UV-visible spectra. The XRD

data indicates that the size of the $Ag@TiO_2$ nanocomposite is in the order of 36 nm. The photocatlytic activity result shows that the silver doped TiO_2 is more efficient than undoped TiO_2 at photocatalytic degradation of methylene blue dye in aqueous stream. Degradation tests were further carried out in the presence of hydrogen peroxide with and without photocatalyst. 93.7 % of methylene blue dye was degraded in the presence of $Ag@TiO_2$ and H_2O_2 in 1 hr as compared to 58.04% degradation in the presence of H_2O_2 only under similar conditions.

References

[1] L. Miao, S. Tanemura, S. Toh, K Kaneko, and M. Tanemura, Appl. Surf. Sci. 238 (2004) 175-179.

[2] C. Xu, Y. Zhan, K. Hong, and G. Wang, Solid State Commun. 126 (2003) 5 Miao 45-549.

[3] B. Cheng, J.M. Russell, W. Shi, L. Zhang, and E.T. Samulski, J. Am. Chem. Soc. 126 (2004) 5972-5973.

[4] M. Adachi, Y. Murata, M. Harada, and S. Yoshikawa, Electrochemistry. 70 (2002) 449-452.

[5] S. Pavasupree, Y. Suzuki, S. Pivsa-Art, and S. Yoshikawa, Sci. Tech. Adv. Mater. 6 (2005) 224-229.

[6] C. He, Y. Yu, X. Hu, and A. Labort, Appl. Surf. Sci. 200 (2001) 239-247.

[7] Ashutosh Tiwari, Shaoqin Gonga, Electroanalysis, 20 (2008) 1775.

[8] I.M. Arabatzis, T. Stergiopoulos, M.C. Berned, D. Labou, S.G. Neophyteds, Appl. Catal. B. Environ. 42 (2003) 187.

[9] E. Stathatos, T. Petrova, P. Lianos, Langmuir 17 (2001) 5025.

[10] C.Y Chen and W.H. Taun, J, Am. Cerm, Soc. 83 (2000) 2988.

[11] H.R. Prakash Naik, H.S. Bhojya Naik, P.J. Bindu, T. Arvinda, D.S Lamani, Medicinal Chemistry. 5 (2008) 148-157

[12] I. Pastoriza-Santos, D.S. Koktysh, A.A. Mamedov, M. Giersig, N.A. Kotov, L.M. Liz-Marzan, Langmuir. 16 (2000) 2731-2735.

[13] R. Jang, R. Vittal, K.J. Kim, Langmuir. 20 (2004) 9807-9810.

[14] M.R. Hoffman, S.T. Martin, W. Choi, W. Bahnemann, Chem. Rev. 95 (1995) 69-96

[15] A. Tiwari, J. Macrom. Sci. A, 2007, 44, 735–745

[16] C.C. Chen, X.Z. Li, W.H. Ma, J. Phys. Chem. B. 106 (2002) 318.

[17] S. Malato, J. Blanco, C. Richter, B. Braun., and M. I. Maldonado. Appl. Catal.B. 17 (1998) 347-356

.